Numerical Investigation of the Effect of Cooled EGR on Turbocharger HCCI Engine Performance Fueled with Methane

T.OUKSEL, A.CHELGHOUM, A. MAMERI

Department of Mechanical Engineering, Faculty of Science and Applied Science, Oum EL Bouaghi University, BP 358, 04000, Algeria

ouksel@yahoo.fr

Abstract

In this paper the work deals with the computational analysis of early direct injected HCCI engine with turbocharger using the CHEMKIN-PRO software [1]. Since controls of combustion phenomenon and ignition timing are the main issues of these engines, the effects of cooled EGR as the controlling factors on the operating parameters such as in-cylinder temperature and pressure of HCCI engines are explored. The cooled EGR was constituted by CO2, H2O, N2, O2. The aim with the EGR was to study the differences caused by the addition of species that could enhance combustion. EGR was introduced in CHEMKIN-PRO simulations, varying it from 0% to 40%. The quantities of the components present in EGR were calculated by running a simulation in CHEMKIN-PRO with only air and fuel and analyzing the mol fractions produced of the gases in which the interest rely.

Since pressure and temperature profiles plays a very important role in reaction path at certain operating conditions, an attempt had been made here to present a complete reaction path investigation on the formation/destruction of chemical species at peak temperature and pressure conditions in the first, middle and last zone.

Keywords: *CHEMKIN-PRO software, Multi-Zone Model, cooled EGR, methane, chemical kinetics, HCCI combustion, emission*

1. Introduction

Homogeneous Charge Compression Ignition (HCCI) Engines is a form of internal combustion in which the fuel and air are compressed to the point of auto ignition. That means no spark is required to ignite the fuel/air mixture creates the same amount of power as a traditional engine, but uses less fuel. HCCI incorporates the best features of both spark ignition (SI) and compression ignition (CI). It is an SI engine, the charge is well mixed, which minimizes particulate emissions and it is an CI engine, the charge is compression ignited and has no throttling losses, which leads to high efficiency. The combustion with HCCI is a given concentration of fuel and air will spontaneously ignite when it reaches its auto-ignition temperature, so it with Homogeneous mixture, homogeneous combustion and absence of flame propagation, simultaneous oxidation of the entire charge, unlike conventional engines, the combustion occurs simultaneously throughout the volume rather than in a flame front. This important attribute of HCCI allows combustion to occur at much lower temperatures; dramatically reducing engine-out emissions of NOx.

Because EGR serves two purposes in HCCI engines, adding thermal energy to the uncompressed mixture and acting as an energy sink to slow oxidation kinetics, it is widely used for extending the HCCI operating range [2, 7, 8, 9, 11 and 12]. Since the earliest studies by Kong et al [22], conducted experiments on a Single Cylinder Oil Test Engine (SCOTE) and operated in a premixed mode using an early fuel injection scheme with two different direct injection systems using diesel fuel. The change in the combustion phasing due to high levels of EGR was also well predicted by the model, which showed that the ignition delay and combustion duration increased with increased EGR percentages. Sjoberg et al [23], conducted experiments on a single-cylinder HCCI research engine (0.98 liters) with a compression ratio 14. This work explores how the high-load limits of HCCI are affected by fuel auto-ignition reactivity,

[DOI: 10.22068/ijae.7.1.2300]

EGR quality/composition, and EGR unmixed for naturally aspirated conditions. This is done for the fuels PRF80 and PRF60 and experimental results are compared among them and found that the fuel PRF 80 is better as far as emissions are considered. Li et al [24], conducted experiments on a single cylinder Co-operative Fuel Research (CFR) engine. They found emission characteristics of a HCCI engine operation using n-heptane as fuel. The effect of intake temperature, air fuel ratio, compression ratio, turbo-charging, and EGR rate on exhaust emissions were explored. The analysis of the exhaust gases included oxides of nitrogen (NOx), carbon monoxide (CO), hydrocarbon emissions (HC), and soot. The hydrocarbon species present in exhaust gases and their concentrations at several operating conditions were also characterized. The approaches to retard HCCI combustion phase without deteriorating combustion efficiency are examined.

Ryan et al [25], conducted experiments on a variable compression ratio single cylinder HCCI engine using diesel. The experimental variables, in addition to speed and load, included compression ratio, EGR level, intake manifold pressure and temperature, fuel introduction location, and fuel composition. The effects of the independent variable on the start of reaction have been documented. The EGR affects these relationships in complex interactions with intake manifold temperature and pressure, and overall air fuel ratio. Olsson et al [26], investigated the effect of cooled EGR on a turbo charged multi cylinder HCCI engine. A six cylinder, Scania D12 truck engine is modified for HCCI operation. It is fitted with port fuel injection of ethanol and n-heptane and cylinder pressure sensors for closed loop combustion control. During idle, low speed and no load, the focus is on the effects on combustion efficiency, emissions of unburned hydrocarbons and CO. At high loads, the focus is on boost pressure to reduce NOx emissions and the ability to run the engine at high mean effective pressure without exceeding the physical constraints of the engine. In this case the effect of EGR on boost pressure, combustion duration and phasing are of primary interest. It is shown that CO, HC and NOx emissions in most cases all improve with EGR compared to lean burn.

In this paper a Multi-zone detailed chemistry combustion model has been implemented into the direct injected HCCI engine with turbocharger fueled with Methane using 40 zones. The model utilizes the library of CHEMKIN-PRO software for determining chemical production rates. The system of equations solved in the Multi-zone HCCI combustion model, is based on a fixed mass, variable volume reactor. With considering extended Zeldovich mechanism, the overall mechanism involves 325 chemical reactions and 53 species. As a result, the effect of cooled EGR on the characteristics of auto-ignition, rate of heat release, and performance characteristics of the HCCI engine and emission have been investigated. Since pressure and temperature profiles plays a very important role in reaction path at certain operating conditions, an attempt had been made here to present a complete reaction path investigation on the formation/destruction of chemical species at peak temperature and pressure conditions, in the first zone (Zone #1), middle zone (Zone #20) and last zone (Zone #40).

2. Model Description

The cylinder volume is divided into a 40 of imaginary zones according to the in cylinder distribution of a variable, normally gas temperature. The multi-zone model treats each zone as a closed homogeneous reactor, where the zone mass is conserved. Pressure is assumed to be the same for all zones and the total volume of all zones is equal to the instantaneous volume of the cylinder. Heat transfer between zones is not considered. The only interaction between zones is through pressure work; if combustion takes place within a zone, it expands to exert work on the other zones [15].

3. Governing Equations

Since the zones are treated as variable-volume closed homogeneous reactors, governing equations for species and temperature of individual zones are the same as those employed by the single-zone HCCI engine model [15]:

3.1 Species

$$\rho^{i}.\frac{dY_k^i}{dt} = \dot{w}_k^i.W_k \quad , \quad \text{for } i=1,\ldots,N_{zone}$$

Where ρ^i is the zone density and Y_k^i, Wk and ẇ_k^i are the mass fraction, molecular weight, and molar production rate of the kth species. The superscript "i" in the equation denotes the zone index and Nzone is the number of zones used by the multi-zone model analysis (Nzone = 40).

3.2. Internal Energy/Temperature

The zone temperature may be determined in two ways. When the crank angle is less than a pre-defined **transition crank angle**, θt, the zone temperature is

[DOI: 10.22068/ijae.7.1.2300]

obtained from a temperature profile extracted from a CFD solution:

$$T^i = T^i_{profile}(t) \qquad \theta(t) \leq \theta \qquad (2)$$

In the above equation, $\theta(t)$ is the crank angle at time *t* and $T^i_{profile}(t)$ is the temperature versus time profile for zone *i*. The temperature profile option allows the multi-zone model to take advantage of the more precise zone temperature histories predicted by third-party CFD software when heat release from chemical reactions is not significant. After the transition angle is reached, the zone temperature will be solved by the zone energy equation:

$$\rho^i . C_v^i . \frac{dT^i}{dt} = -\sum_{k=1}^{k_{gas}} \dot{w}_k^i . W_k . u_k^i - \frac{P^i}{V^i} . \frac{dV^i}{dt} - \frac{h_w^i . (T^i - T_w) . A_w^i}{V^i} \quad , \quad \theta(t) > \theta_t \qquad (3)$$

Where, P, T, and V are zone pressure, temperature and volume, respectively. C_v is the constant-volume specific heat capacity of the gas mixture comprising the zone and u_k is the internal energy of the k_{th} species. h_w *and* A_w are zone wall heat transfer coefficient and zone wall surface area, respectively. The CHEMKIN-PRO multi-zone model assumes zone wall surface area is a constant fraction of the total cylinder wall surface area (see tableau 2). The wall heat-transfer coefficient is computed by the **modified Woschni** heat-transfer correlation **[10]**.

Where, P, T, and V are zone pressure, temperature and volume, respectively. Cv is the constant-volume specific heat capacity of the gas mixture comprising the zone and uk is the internal energy of the kth species. hw and Aw are zone wall heat transfer coefficient and zone wall surface area, respectively. The CHEMKIN-PRO multi-zone model assumes zone wall surface area is a constant fraction of the total cylinder wall surface area (see tableau 2). The wall heat-transfer coefficient is computed by the modified Woschni heat-transfer correlation [10].

3.3. Volume/Accumulated Volume

In the multi-zone model, the cylinder volume is computed by the slider-crank relationship used in the single-zone internal-combustion engine model. Individual zone volume is not known and needs to be solved. Since gas composition and temperature in each zone are solved by their corresponding governing equations, zone pressure and volume are coupled by the equation of state, i.e., ideal gas law.

In order to solve the system of equations more efficiently, a new variable is introduced

$$G^i = \sum_{j=1}^{i} P^j . V^j$$

Since pressure is the same in all zones, the G variable can be considered as a pressure-weighted accumulated zone volume. The use of pressure as scaling factor helps minimize the variation of G variable during the engine cycle. In addition, by replacing zone volume, V, with the G variable, the Jacobian matrix becomes banded along the diagonal and the system of equation can be integrated more effectively. The zone volume can be converted from the G variable by

$$V^i = \frac{G^i - G^{i-1}}{P^i} \qquad (5)$$

The governing equation for the new *G* variable can be derived from the equation of state as

$$G^1 = P^1 . V^1 = M^1 . R . T^1 . \sum_{k=1}^{k_{gas}} \frac{Y_k^1}{W_k} \quad , \text{for i=1} \qquad (6)$$

And, according to the definition of *G*

$$G^i = G^{i-1} + P^i . V^i = G^{i-1} + M^i . R . T^i . \sum_{k=1}^{k_{gas}} \frac{Y_k^i}{W_k} \quad , \text{for i=1} \qquad (7)$$

Where *R* is the universal gas constant and $M^i = \rho^i . V^i$ is the gas mass of zone *i*.

3.4. Cylinder pressure

The assumption of uniform pressure among all zones serves a constraint and provides coupling between the zones

$$P^i = P^{i+1} \text{ , for } i = 1, \ldots, N\text{zone}-1. \qquad (8)$$

To close the pressure equation, the volume constraint

$$V_{cylinder} = \sum_{i=1}^{N_{zone}} V^i \qquad (9)$$

is used to determine the pressure of the last zone ($i = N_{zone}$).

By substituting Equation (8) and Equation (9) into Equation (4) for $i = N_{zone}$, the governing equation for the pressure in the last zone can be obtained

$$P^{Nzone} = \frac{G^{Nzone}}{V_{cylinder}} \qquad (10)$$

Where $V_{cylinder}$ is the instantaneous cylinder volume.

The instantaneous cylinder volume can be determined using slider-crank relations from **[18]**, engine geometry, and the crank angle degree at which the volume is desired to be calculated

[DOI: 10.22068/ijae.7.1.2300]

$$V_{cylinder}(\theta) = V_C.(1+\frac{r_c-1}{2}.\left(R+1-\cos(\theta)-\sqrt{R^2-sin^2(\theta)}\right)) \quad (11)$$

Where R is the ratio of the connecting rod length to the crank arm radius, V_c is the clearance volume and r_c is the compression ratio.

The CHEMKIN-PRO multi-zone model solves Equation (1) - Equation (3), Equation (6) - Equation (8) and Equation (10) for all zones fully-coupled to obtain zone properties. Average properties such as temperature and species concentrations are derived from their zone values.

3.5. Heat transfer model

The dominant heat transfer mechanism in the HCCI engine is forced convection from the bulk gas to combustion chamber walls. The radiation effect is very small because of low-soot, low temperature combustion of the premixed lean mixture in a typical HCCI engine. Among the existing heat transfer models suggested for IC engines, the modified Woschni model is used in this analysis because of its simplicity and wide acceptance**.** The empirical constants of modified Woschni equation in this study have been derived from reference **[10].**

The modified heat transfer coefficient formula proposed by Assanis, D. **[10]** with inclusion of the above mentioned modifications:

$$h_{new}(t) = \alpha_{scaling}.L(t)^{-0.2}.P(t)^{0.8}.T(t)^{-0.73}v(t)_{tuned}^{0.8} \quad (12)$$

$$v(t)_{tuned} = C_1.\bar{S}_p + \frac{C_2}{6}.\frac{V_d.T_r}{P_r.V_r}.(P-P_{motored}) \quad (13)$$

Where $C_1 = (C_{11} + C_{12}.\frac{V_{swirl}}{\bar{S}_p})$

And $\bar{S}_p$ is the mean piston speed.

Here, C_{11} , C_{12} , and C_2 are modeling parameters, V_{swirl} is the swirl velocity, V_d is the displacement volume, P and P_{mot} are instantaneous pressure and the corresponding motoring pressure at the same firing condition, and T_r, P_r and V_r are temperature, pressure and volume at the IVC moment.

Equations (12) and (13) represent the modified heat transfer coefficient formula with inclusion of the above mentioned modifications.

The modified model **[10]**.has three differences from the original Woschni model **[21]**: $L(t)$ the instantaneous chamber height is used as the characteristic length scale, the temperature exponent is modified to be 0.73, and C_2 is reduced to 1/6 of the original value.

4. Chemical kinetics model

The rates of creation/destruction of chemical species are modeled using mass-action kinetics and the specific reaction rate constants strongly depend on the temperature.

solving complex chemical kinetics problems and allows the user to calculate species concentrations, heat release rate, temperature and pressure history of the combustion.

An elementary reaction that involves *K* chemical species in *i* reactions can be represented in the form of:

$$\sum_{k=1}^{K} \upsilon'_{ki}\cdot\chi_k \Leftrightarrow \sum_{k=1}^{K} \upsilon''_{ki}\cdot\chi_k \quad (14)$$

$$\dot{w}_k^i = (\upsilon''_{ki}-\upsilon'_{ki}).q_i \quad (15)$$

$$q_i = k_{f,i}.\prod_{k=1}^{K}[X_k]^{\upsilon'_{ki}} - k_{r,i}\prod_{k=1}^{K}[X_k]^{\upsilon''_{ki}} \quad (16)$$

Where υ_{ki}, χ_k, $\dot{w}_k^i$, q_i, $k_{f,i}$ and $k_{r,i}$ are the stoichiometric coefficients, the chemical symbol for the k_{th} species, the production rate of the k_{th} species, the rate of progress variable for the i_{th} reaction, the forward and reverse rate constants of the *i*th reaction, respectively.

The forward and reverse rate constants of the i_{th} reaction rate could be expressed as:

$$k_{f,i} = A_i.T^{\beta_i}.exp\left(\frac{-E_i}{R_c.T}\right) \quad (17)$$

$$k_{r,i} = \frac{k_{f,i}}{K_{c,i}} \quad (18)$$

$$K_{c,i} = K_{p,i}.\left(\frac{P_{atm}}{R.T}\right)^{\sum_{k=1}^{K}(\upsilon''_{ki}-\upsilon'_{ki})} \quad (19)$$

$$K_{p,i} = exp\left(\frac{\Delta S_0^i}{R}-\frac{\Delta H_0^i}{R.T}\right) \quad (20)$$

Where *Ai*, *βi*, E_i and $K_{p,i}$ are the pre-exponential factor, the temperature exponent, the activation energy and the equilibrium constants, respectively.

4.1. Thermodynamic property treatment

The working fluid composition in the cylinder is constantly changed. Once at any time the composition is determined, mixture properties can be calculated. This method simply considers thermodynamic properties of the mixture containing residual gas, exhaust gas recirculation, unburned gaseous fuel and air. For thermodynamic properties such as constant pressure specific heat, enthalpy and entropy, the NASA curve fits in the following forms are used **[16]**:

$$\frac{C_{pk}^0}{R} = \sum_{n=1}^{5} a_{nk}.T^{n-1} \quad (21)$$

$$\frac{h_k^0}{R.T} = a_{1k} + \sum_{n=1}^{5}\frac{a_{n,k}}{n}.T_k^{n-1} + \frac{a_{6k}}{T_k} \quad (22)$$

$$\frac{s_k^0}{R} = a_{1k}.lnT_k + \sum_{n=1}^{4}\frac{a_{n+1,k}}{n}.T_k^n + a_{7k} \quad (23)$$

5. CHEMKIN-PRO Set Up

The package used to model combustion and chemical kinetics of the HCCI combustion is called CHEMKIN Pro. This software is one of the most known packages for

[DOI: 10.22068/ijae.7.1.2300]

Before the start of modeling in CHEMKIN a pre process is required. This pre process will check if the basics to run the desired simulations are present.

The two sets of data that need to be pre processed prior to the actual modeling are the gas-phase kinetics input and the species thermodynamic data without each, no complete information is available to run the chemical kinetic equations. On the gas-phase kinetic input data, all the chemical elements and species are accounted for, and every reaction between them is shown with the correspondent reaction rate coefficients. These chemistry sets can be prepared by the user or can be obtained from different resources, namely previous work done by other researchers.

The chemical kinetic mechanism used in this paper incorporated the GRIMECH-3.0 mechanism **[19]** that considers **53** species and **325** reactions, including NOx chemistry. The other file that requires pre process is the thermodynamic data. On this file all the information regarding thermodynamic properties of the species involved on every reaction are specified. Again this file can be built by the user using thermodynamic data as information or complete sets developed already can be used.

The next stage of the modeling process is where a specific reactor is selected to cope with the demands of the desired simulation.

The CHEMKIN input for the simulation was based on the HCCI model that the package from Reaction Design, already includes.

The input parameters used were **[20]**; number of engine angle degrees to be calculated, 300 degrees; engine compression ratio, 10.5; engine displacement volume, 1378 cm^3; engine connecting rod to crank radius, 2.7871; engine speed, 2007 rpm; start crank angle, -155°; temperature at IVC, 573 K; pressure at IVC, 3.18 bar; equivalence ratio, 0.4; heat transfer correlation, a=0.035, b=0.73, c=0.0; chamber bore diameter, 11.41 cm; stroke, 13.5 cm; wall temperature, 424 K; Woschni correlation of average cylinder gas velocity, C_{11}=2.28, C_{12}=0.308, C_2=3.24.10^{-3}; ratio of swirl velocity, 0.0.

6. Results and Discussion

6.1. Engine specifications

The experimental data is taken from **[20].** The engine specifications are listed in **Table 1**.

Zone numbering is considered in an ascending order from the combustion chamber wall to the core in-cylinder region (i.e., from zone #1 with the lowest temperature to zone #40 with the highest temperature).

Table 2 shows the zone temperature distribution. Zones #1 to #12 represent the crevices. Zones #13 to #22 represent the boundary layer. The core region is represented by zones #23 to #40.

The simulations with EGR show peak pressures and temperatures decreasing as EGR rates increase (Fig.1 and Fig .2). This is a clear result of the increase in mixture specific heats as more CO2 and H2O are added.

Fig.3 shows that increasing EGR has the effect of retarding the start of combustion and increasing its duration. The first effect is a consequence of the higher heat capacity of the exhaust gas, which delays the mixture from reaching the conditions to initiate the cool flame combustion. Furthermore, increasing EGR reduces the oxygen concentration, which decreases the reaction rate.

Temperature profiles of individual zones predicted by the CHEMKIN multi-zone simulation are shown in Fig.4 together with the average temperature. The transition angle is set to 15.5□ degrees BTDC as given by Aceves et al [20]. As we can see from Figure 4 the temperature decreases from zone 40 (core) to zone 1 (crevice).

Figure 5 shows the maximum gas pressure (Pmax) averaged including 40 zones vs rate of EGR (%). It is seen that, Pmax decrease as rate of EGR increase from 0 % to 40 % . The reason for this can be attributed to the fact that the higher heat capacity of the exhaust gas, which delays the mixture from reaching the conditions to initiate the cool flame combustion.

Figure 6 shows the maximum gas temperature (Tmax) averaged including 40 zones vs rate of EGR (%). It is seen that, Tmax decrease as EGR increase from 0 % to 40 % . The reason for this can be attributed to the fact that the EGR acting as energy sink to slow oxidation kinetics.

Figures 7, 8 and 9 shows the variation of the net heat release rate per CA_zone for zones 1, 10, 20, 30 ,40 and averaged zone vs crank angle for 0% EGR, 20 % EGR and 40 % EGR respectively. It is seen that, the total burn duration increased significantly with EGR rate, but SOC had little or no dependence on EGR rate. The peak of NHRR per CA decrease rapidly when the rate of EGR increase from 0% to 40 % . It can see that combustion starts from hot ignition zones in the center of the chamber (zone 40) where temperature is higher and then proceeds to the whole chamber (zone 1).

Figures 10 and 11 shows mole fraction of NO per CA histories for 0 % EGR, 20 % EGR respectively. These figures show that increasing amount of EGR reduce the NO emissions up to 94 % less than that without EGR. The reason for this can be attributed to the fact that EGR decreases the heat release rate, and hence lowers the maximum cylinder temperature due to the constituents of EGR (primarily CO2 and H2O) having higher specific heat capacities.

Figures 12, 13 and 14 shows the reaction path of the turbocharger HCCI engine at peak temperature for zones 1, 20 and 40 respectively. The thicker arrows represent the major reaction path and the thinner arrows represent the minor reaction path. As we can see from figures 13, 14, the combustion is complete because the end products are carbon dioxide (CO2) and water vapour (H2O). In this reaction path it is clear that hydrogen oxide (OH) and hydroperoxy (HO2) are the major contributors for the formation of water vapour (H2O). The components like carbon monoxide (CO), hydrogen oxide (OH) contributes to the formation of carbon dioxide (CO2).

Table 1. Engine parameters and operating conditions used in the analysis [20].

[DOI: 10.22068/ijae.7.1.2300]

Parameter	Value
Engine speed	2007 rpm
Compression ratio	10.5:1
Stroke	13.5 cm
Bore	11.41 cm
Connecting rod length	21.6 cm
Displacement volume	1378 cm3
Crank angle at intake valve closing (IVC)	-155°
Chemical kinetic mechanism	GRI-MECH 3.0
Fuel	Methane
Pressure at IVC	3.18 bar
Temperature at IVC	573 K
Average equivalence ratio	0.4
Residual gas fraction	2%

Table 2. Zone configuration used by the multi-zone model analysis for the validation case**.** This mass distribution is based on the results in **[15]** and is modified suitably.

Zone#	1	2	3	4	5	6	7	8	9	10	11	12	13	14	15	16	17	18	19	20
Region	Crevice												Boundary							
Mass%	0.5	0.5	0.5	0.5	0.5	0.5	0.5	0.5	0.5	0.5	0.5	0.5	1	1	1.5	1.5	1.5	1.5	2	2
Area%	1.5	1	1.5	1	1.5	1	1.5	1	1.5	1	1.5	1	2.5	2	2.5	3	3	2.5	2	2.5
Zone#	21	22	23	24	25	26	27	28	29	30	31	32	33	34	35	36	37	38	39	40
Region	Layer		Core																	
Mass%	2	2	3	3	3	3	3	3	3	3	4.5	4.5	4.5	4.5	5.5	5.5	5.5	5.5	7	7
Area%	3.5	4	3.5	4	3.5	4	3.5	4	3.5	4	3.5	4	2.5	2.5	2.5	2.5	2.5	2.5	2.5	2.5

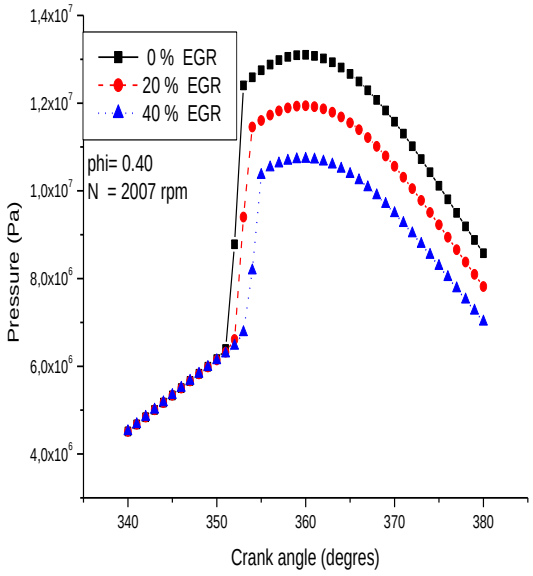

Fig1.. In cylinder pressure variation for three different EGR rate

[DOI: 10.22068/ijae.7.1.2300]

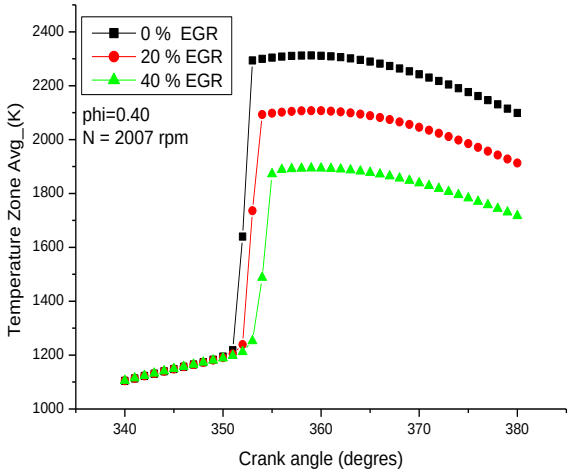

Fig2. In cylinder temperature variation for three different EGR rate

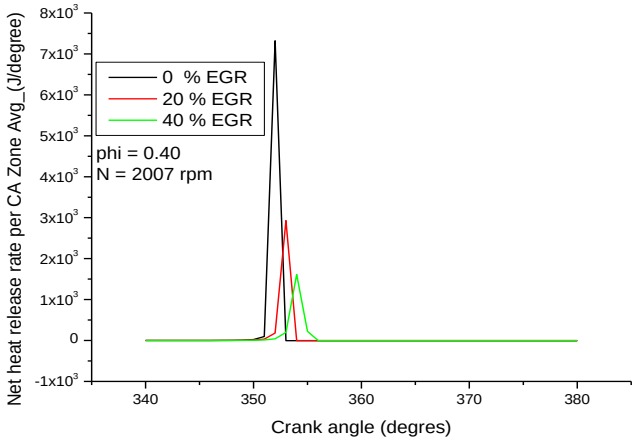

Fig3.. Variation of the NHRR per CA_Zone Average for three different EGR rate

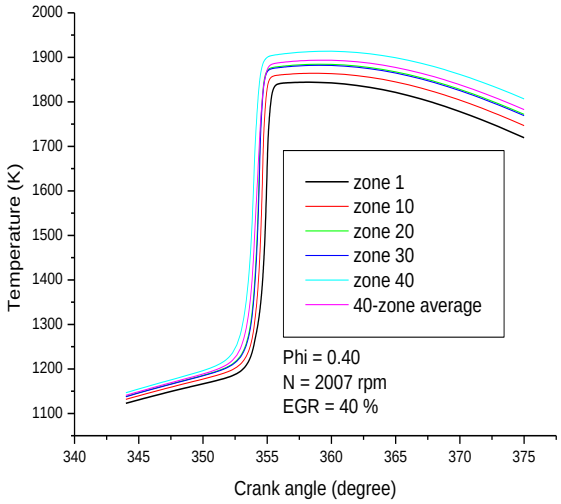

Fig4. Temperatures predicted by the multi-zone model. The energy-equation is engaged at -15.5° BTDC.

[DOI: 10.22068/ijae.7.1.2300]

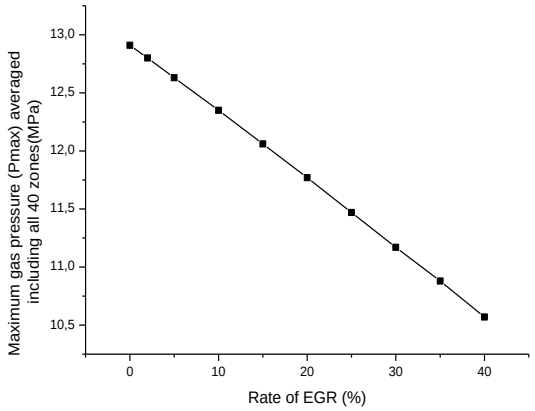

Fig5. Maximum gas pressure (Pmax) averaged including 40 zones vs rate of EGR (%)

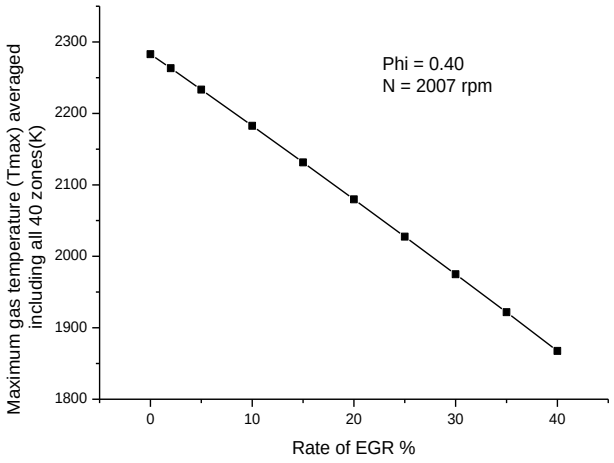

Fig6. Maximum gas temperature (Tmax) averaged including 40 zones vs rate of EGR (%)

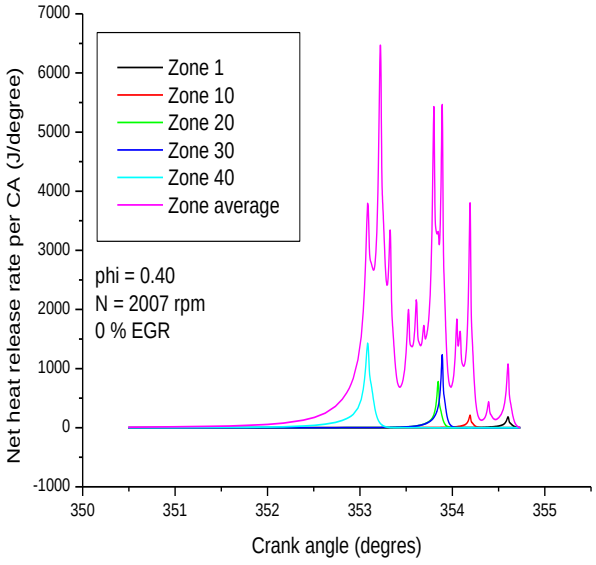

Fig7. Zone NHRR per CA histories without EGR

[DOI: 10.22068/ijae.7.1.2300]

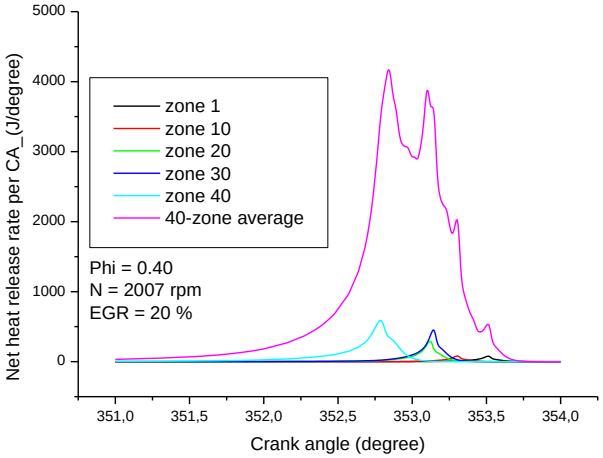

Fig8. Zone NHRR per CA histories with 20 % EGR

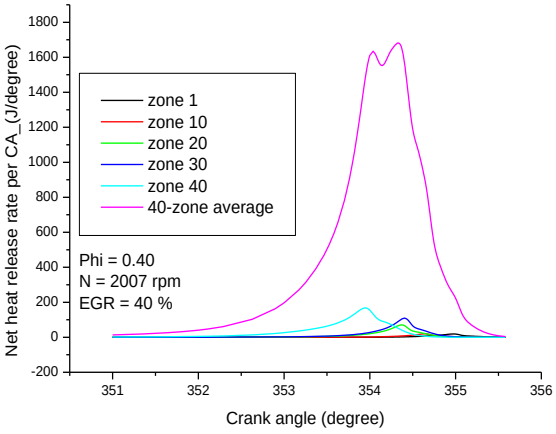

Fig9. Zone NHRR per CA histories with 40 % EGR

[DOI: 10.22068/ijae.7.1.2300]

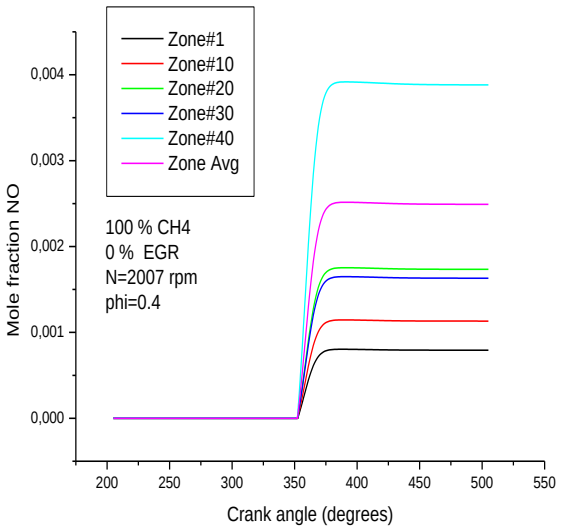

Fig10. . Mole fraction of NO per CA histories (100 % CH4/0% EGR, phi = 0.40)

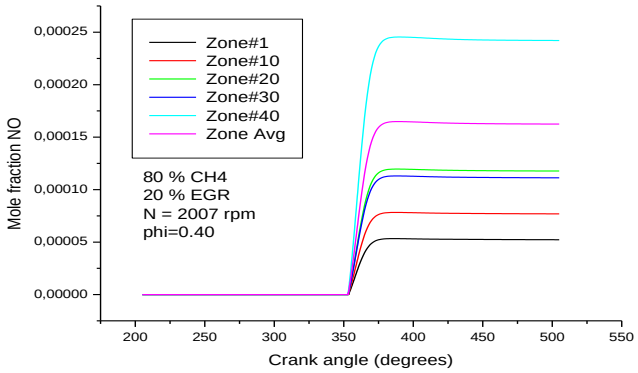

Fig11. Mole fraction of NO per CA histories (80 % CH4/ 20% EGR, phi = 0.40)

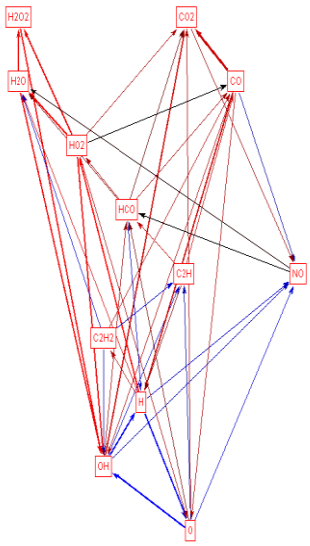

Fig12. Reaction path of the turbocharger HCCI engine at peak temperature for zone 1(crevices), (phi = 0.40; 40 % EGR; Tmax_zone1 = 1844.156 K; N = 2007 rpm)

[DOI: 10.22068/ijae.7.1.2300]

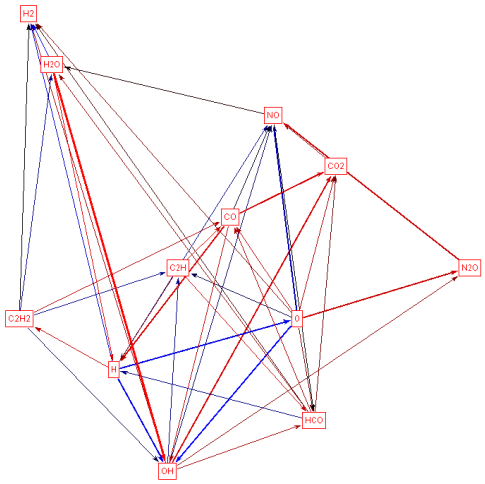

Fig13. Reaction path of the turbocharger HCCI engine at peak temperature for zone 20 (boundary layer), (phi = 0.40; 40 % EGR; Tmax_zone20 = 1884.625 K; N = 2007 rpm)

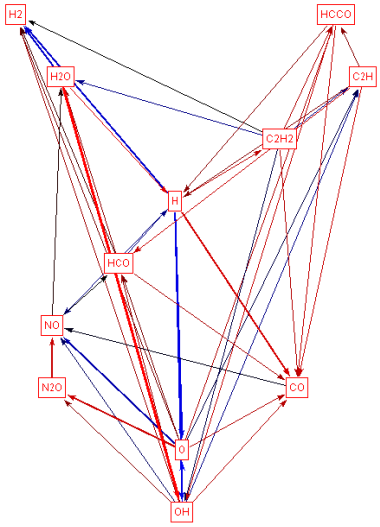

Fig14. Reaction path of the turbocharger HCCI engine at peak temperature for zone 40 (core), (phi = 0.40; 40% EGR; Tmax_zone40 = 1913.727 K; N = 2007 rpm)

6. Conclusion

In this work, the numerical investigation of the effect of cooled EGR on turbocharger HCCI engine performance fuelled with methane are studied using the CHEMKIN-PRO software.

For this purpose, a Multi-zone thermo-kinetic model was used with 40 zones.

The results of this study can be summarized as below:

The combustion starts from hot ignition zones in the center of the chamber (zone 40) where temperature is higher and then proceeds to the whole chamber (zone 1).

With increasing amounts of EGR from 0% to 40 % the combustion process becomes slower, resulting in lower peak pressure and temperature, lower rate of heat release and therefore longer combustion rates.

By turbocharged operation the peak temperature and peak pressure of the combustion are substantially increased when compared to normal HCCI combustion without turbocharger.

[DOI: 10.22068/ijae.7.1.2300]

As the main source of NOx in HCCI engine is concerned to thermal NOx, adding EGR to natural gas would decrease engine NOx emissions because the maximum cylinder temperature and high temperature duration would decrease by additing EGR.

There is an optimum value of additive for each operating condition, which results in higher engine power and less NOx (increasing amount of EGR from 0%, to 40% reduce the NO emissions up to 94 % less than without EGR). This optimum value is 20 % EGR.

HCCI is a combustion concept which is developed in response to the need of lower NOx & soot emission and Efficiency. It can substantially overcome both the problems but still it needs a lot of development.

. Nomenclature

HCCI Homogeneous Charge Compression Ignition
EGR Exhaust Gas Recirculation
SI Spark Ignition
CI Compression Ignition
SOC Start Of Combustion
BTDC Before Top Dead Center
CAD Crank Angle Degrees
NHRR Net Heat Release Rate
TDC Top Dead Center
IVC Intake Valve Closing
EVO Exhaust Valve Opening
Phi Equivalence ratio
NOx Oxides of Nitrogen
CO Carbon monoxide
HC Unburned Hydrocarbon
SCOTE Single Cylinder Oil Test Engine
CFR Co-operative Fuel Research engine

References

[1]. CHEMKIN-PRO 15131, Reaction Design, San Diego, CA, 2013.
[2]. Nakamura Y., Jung D.W., and Iida N., "Closed-loop combustion control of a HCCI engine with re-breathing EGR system", SAE paper 2013-32-9069, 2013.
[3]. Nobakht, A., et al., "A Parametric Study on Natural Gas Fueled HCCI Combustion Engine Using a Multi-Zone Combustion Model", Fuel, 90 (2011), 4, pp. 1508-1514
[4]. "Modeling HCCI Engine with Exhaust Gas Recirculation", Application Note: CHEMKIN-PRO, PRO-APP-Auto-7 (v2.0) August 30, 2010.
[5]. Yao, M., et al., "Progress and Recent Trends in Homogeneous Charge Compression Ignition (HCCI) Engines", Prog. Energ. Combust., 35 (2009), 5, pp. 398-497
[6]. Handford, D. I., Checkel,M. D., "Extending the Load Range of a Natural Gas HCCI Engine using Direct Injected Pilot Charge and External EGR", SAE technical paper 2009-01-1884, 2009
[7]. [7] M. Shahbakhti, and C. R. Koch. "Thermo-Kinetic Combustion Modeling of an HCCI Engine to Analyze Ignition Timing for Control Applications". Proceeding of Combustion Institute/Canadian Section (CI/CS) Spring Technical Conference, 2007.
[8]. Ohmura, T., et al., "A Study on Combustion Control by Using Internal and External EGR for HCCI Engines Fuelled with DME", SAE technical paper 2006-32-0045, 2006.
[9]. Dubreuil A, Foucher F, Mounaim-Rousselle C, "Effect of EGR Chemical Components and Intake Temperature on HCCI Combustion Development", SAE 32 (2006).
[10]. Assanis, D., Chang, J., Güralp, O. and Filipi, Z. "New Heat Transfer Correlation for an HCCI Engine Derived from Measurements of Instantaneous Surface Heat Flux", SAE Papers, NO. 2004-01-2996.
[11]. Babajimopoulos, A., Lavoie, G.A., Assanis, D.N., "Modeling HCCI Combustion with High Levels of Residual Gas Fraction - A Comparison of Two VVA Strategies," SAE Paper 2003-01-3220, 2003.
[12]. Abd-Alla G.H.: "Using exhaust gas recirculation in internal combustion engines: a review", Energy Conversion Management 43, 1027-1042 (2002).
[13]. Flowers D, Aceves S, Westbrook CK, Smith JR, Dibble R., "Detailed chemical kinetic simulation of natural gas HCCI combustion: gas composition effects and investigation of control strategies". J Eng Gas Turbine Power 2001;123:433–9.
[14]. Aceves, S. M., Flower, D., L., Martinez, F. and Smith, R., "HCCI Combustion: Analysis and Experiments." SAE Papers, No. 2001-01-2077.

[DOI: 10.22068/ijae.7.1.2300]

[15]. Aceves, S. M., Flowers, D. L., Westbrook, C. K.,Smith, J. R., Pitz, W., Dibble, R.,Christensen, M., and Johansson, B., "A Multi-ZoneModel for Prediction of HCCI Combustion and Emissions," SAE paper no. 2000-01-0327, 2000.
[16]. Mcbride, J., Reno, A., "Coefficients for calculating thermodynamics and transport properties of individual species," NASA Technical Memorandum 4513, 1999.
[17]. Flowers, D. L., Aceves, S. M., Westbrook, C.K., Smith, J. R., and Dibble, R. W.,"Sensitivity of Natural Gas HCCI Combustion to Fuel and Operating Parameters Using Detailed Kinetic Modeling," In AES-Vol. 39,"Proceedings of the ASME Advanced Energy Systems Division - 1999," edited by S. M. Aceves,S. Garimella and R. Peterson, pp.465-473, 1999.
[18]. Heywood J.B.: "Internal Combustion Engine Fundamentals", McGraw-Hill, Inc., New York (1988).
[19]. http://www.me.berkeley.edu/gri-mech/version30/text30.html.
[20]. S. M. Aceves, D. L. Flowers, F. Espinosa-Loza, A.Babajimopoulos, D. N. Assanis "Analysis of Premixed Charge Compression Ignition Combustion with a Sequential Fluid Mechanics-Multizone Chemical Kinetics Model ", 2005 SAE World Congress Detroit, MI, United States
[21]. [21] Woschni, G., "Universally Applicable Equation for the Instantaneous Heat Transfer Coefficient in the Internal Combustion Engine," SAE Paper 670931, 1967.
[22]. Kong S., C., Marriott, C. D., Rutland, C. J., and Reitz, R. D., "Experiemnts and CFD Modeling of Direct Injection Gasoline HCCI Engine Combustion," SAE paper 2002-01-1925.
[23]. Sjöberg, M., Edling, L.-O., Eliassen, T., Magnusson, L., and Angström, H.-E., "GDI HCCI: Effects of Injection Timing and Air Swirl on Fuel Stratification, Combustion and Emissions Formation," SAE Paper 2002-01-0106, 2002.
[24]. Li, J., Zhao, H., Ladommatos, N., and Ma, T., "Research and Development of Controlled Auto-Ignition (CAI) Combustion in a 4-Stroke Multi-Cylinder Gasoline Engine," SAE paper 2001-01-3608.
[25]. Ryan, T. W., Callahan, T. J., "Homogeneous Charge Compression Ignition of Diesel Fuel," SAE paper 961160.
[26]. Olsson, J., Tunestal, P., and Johansson, B., "Closed-Loop Control of an HCCI Engine,"
[27]. SAE Paper 2001-01-1031.

[DOI: 10.22068/ijae.7.1.2300]